narra j

Original Article

Comparative analysis of hemotoxic, myotoxic, and inflammatory profiles of *Calloselasma rhodostoma* and *Trimeresurus insularis* venoms in mice

Adiva Aphrodita[1], Diva N. Sentono[1], Donan S. Yudha[1], Yekti A. Purwestri[1,2], Tri R. Nuringtyas[1,2], Slamet Raharjo[3], Isra Wahid[4,5], Sri N. Rahmi[4,5], Setyanto T. Wahyudi[6] and Fajar Sofyantoro[1*]

[1]Department of Tropical Biology, Faculty of Biology, Universitas Gadjah Mada, Yogyakarta, Indonesia; [2]Research Center for Biotechnology, Universitas Gadjah Mada, Yogyakarta, Indonesia; [3]Department of Internal Medicine, Faculty of Veterinary Medicine, Universitas Gadjah Mada, Yogyakarta, Indonesia; [4]Department of Parasitology, Faculty of Medicine, Universitas Hasanuddin, Makassar, Indonesia; [5]Center for Zoonotic and Emerging Diseases HUMRC, Faculty of Medicine, Universitas Hasanuddin, Makassar, Indonesia; [6]Department of Physics, Faculty of Mathematics and Natural Sciences, IPB University, Bogor, Indonesia

*Corresponding author: fajar.sofyantoro@ugm.ac.id

Abstract

Snakebite envenomation remains a significant medical concern, particularly in tropical regions where venomous snakes such as *Calloselasma rhodostoma* and *Trimeresurus insularis* are prevalent. Both venoms are known for their potent hemotoxic, myotoxic, and inflammatory effects, yet their differential impacts on systemic physiological pathways remain unclear. The aim of this study was to characterize the hematological, myotoxic, and inflammatory effects of *C. rhodostoma* and *T. insularis* venoms in a murine model and to explore their influence on systemic factors such as insulin-like growth factor 1 (IGF-1), which is critical for muscle repair and inflammation regulation. Mice were exposed to varying doses (20–100 µg) of *C. rhodostoma* and *T. insularis* venoms. Hematological parameters, muscle degeneration, inflammatory cell infiltration, and plasma IGF-1 levels were assessed to evaluate the venoms' systemic and local effects. Our data indicated that *C. rhodostoma* venom induced significant changes in blood coagulation, muscle edema, and inflammatory infiltration, with pronounced effects even at lower doses. Conversely, *T. insularis* venom showed a dose-dependent suppression of IGF-1 levels, highlighting its unique systemic impact. Both venoms caused severe muscle damage, characterized by structural disintegration and increased leukocyte infiltration, with *C. rhodostoma* eliciting a stronger inflammatory response at lower doses.

Keywords: Snakebite envenomation, *Calloselasma rhodostoma*, *Trimeresurus insularis*, hemotoxicity, IGF-1

Introduction

Snakebite envenoming is a neglected tropical disease causing over 100,000 deaths and disabling more than 400,000 people annually, predominantly affecting impoverished rural populations in tropical regions [1,2]. The scarcity of antivenom and delays in its administration contribute to high fatality rates [3,4]. Moreover, snakebite envenoming exacerbates poverty, acting as a significant occupational, environmental, and domestic hazard that perpetuates socioeconomic challenges in affected communities [5,6]. Despite its impact, snakebite has received limited attention from the global health community, with insufficient health programs addressing this

Received: December 4, 2024 - Accepted: March 17, 2025 - Published online: April 21, 2025

issue [5,7]. Recent initiatives by the World Health Organization (WHO) and other organizations have begun to improve awareness and response efforts [7-9]. The high incidence and severe outcomes of snakebites, including in vulnerable groups like children, highlight the urgent need for integrated strategies to improve antivenom access, healthcare, and research to mitigate the global impact of envenoming [10-13].

Understanding snake venom's toxic effects is essential for developing effective antivenoms, which remain the primary treatment for snakebite envenoming [3,14,15]. Venoms contain complex mixtures of toxins that cause neurotoxic, hemotoxic, and myotoxic effects, necessitating rigorous testing of antivenoms to ensure efficacy [4,8,16]. Venom pharmacokinetics, including absorption and clearance, influence antivenom dosing, with variability observed across snake species [17]. Advances in proteomics, transcriptomics, and antivenomics have improved antivenom targeting and effectiveness [14,18]. Pathology-specific and broad-spectrum antivenoms show promise in neutralizing diverse venoms [19,20]. Interest in ethnopharmacological treatments, such as plant-based therapies, complements conventional antivenoms, offering alternative therapeutic options [21,22]. However, venom variability poses challenges for antivenom efficacy, highlighting the need for tailored approaches considering regional and species differences [23,24]. Early antivenom administration can reduce neurotoxic effects, emphasizing timely intervention [25]. Therefore, understanding these dynamics is crucial for advancing antivenom and therapeutic strategies against snakebite envenoming.

Calloselasma rhodostoma and *Trimeresurus insularis* are medically significant venomous snakes known for their potent hemotoxic and myotoxic effects, which contribute to coagulopathy, hemorrhage, and muscle tissue damage in envenomed victims [26,27]. The venom of *C. rhodostoma* is known to cause severe systemic coagulopathy and local tissue injury, as well as nephrotoxicity and cardiovascular disturbances, as demonstrated in animal models [26,28]. The venom's complexity is further highlighted by the diversity of its toxin genes, with snake venom metalloproteinases (SVMPs) being the most dominant, followed by phospholipase A2, C-type lectins, and snake venom serine proteases [29]. Rhodocytin, a toxin from *C. rhodostoma* venom, interacts with the C-type lectin-like receptor 2, leading to local swelling, bleeding, and necrosis, as well as systemic effects on blood coagulation [30]. A clinical trial comparing different antivenoms for *C. rhodostoma* bites has shown varying efficacy in restoring blood coagulability and managing systemic envenoming, with some antivenoms demonstrating superior anti-hemorrhagic and anti-necrotic potency [31]. Meanwhile, a study on the venom composition of *T. insularis* revealed similarities across populations from eight islands in Indonesia, with key protein families including phosphodiesterases, l-amino acid oxidases, P-III snake venom metalloproteinases (SVMP), serine proteases, cysteine-rich secretory proteins, phospholipases A2, and C-type lectins [27]. Comparative proteomic analysis with other Indonesian *Trimeresurus* species, including *T. albolabris*, *T. puniceus*, and *T. purpureomaculatus*, identified 48 proteins from 14 families in *T. insularis* venom, highlighting the compositional variability among species, which is critical for understanding their toxin profiles and developing antivenoms [32]. Another study evaluating the efficacy of Thai green pit viper antivenom (GPVAV) against Indonesian *Trimeresurus* venoms demonstrated strong immunoreactivity and superior neutralization of the lethality and procoagulant effects of *T. insularis* venom compared to the locally used Biosave® *Serum Anti Bisa Ular* (SABU), suggesting GPVAV as a potentially more effective treatment for envenomation by *T. insularis* [33].

Hemotoxins in snake venom significantly disrupt normal blood coagulation, leading to severe complications such as thrombocytopenia, spontaneous bleeding, and disseminated intravascular coagulation [34,35]. These effects result from procoagulant toxins that activate the clotting cascade, causing widespread factor deficiencies commonly observed in envenomation by viperid and some elapid snakes [36-38]. This condition, known as venom-induced consumption coagulopathy (VICC), is a critical systemic syndrome that can result in life-threatening hemorrhage [38,39]. Moreover, hemorrhagic toxins, especially metalloproteinases, directly damage blood vessels through proteolytic degradation of the basement membrane and extracellular matrix around capillaries, leading to both localized and systemic hemorrhages—key complications in snakebite envenomation [40,41]. The interplay between venom components and the human hemostatic system leads to severe hemorrhagic and thrombotic outcomes, involving

the activation of factor X or prothrombin, fibrinogen conversion, and platelet dysfunction [36]. Antivenom remains the primary treatment for snakebite-induced coagulopathy, although its effectiveness varies with snake species and venom composition [38,42]. Meanwhile, snake venom myotoxins, including single-chain peptides and phospholipases A2, are primary contributors to muscle necrosis, leading to severe muscle damage in snakebite victims [43,44]. These toxins disrupt skeletal muscle cell integrity by interacting with the plasma membrane, resulting in vacuolation, cell lysis, and necrosis due to altered membrane permeability [44]. The damage is exacerbated by the release of potassium and ATP from muscle cells, as seen with *Bothrops asper* myotoxins, which intensify muscle damage and pain through purinergic receptor activation [45]. Clinically, venom-induced muscle damage presents as localized soft tissue necrosis and, in severe cases, progresses to rhabdomyolysis and significant loss of muscle-specific proteins [46]. The pathological effects of snake venom are driven by the multifunctional nature of its components, including phospholipases, metalloproteases, serine proteases, and three-finger peptides, which collectively cause inflammation, necrosis, and hemorrhage [47]. Poor muscle regeneration following venom-induced necrosis is often due to microvascular damage that hampers debris clearance and nutrient supply [48]. Additional factors, such as damage to intramuscular nerves, the extracellular matrix, and the persistence of venom in tissues, further impair regeneration [49].

A comprehensive understanding of venom hemotoxicity and myotoxicity is crucial for developing effective therapeutic strategies to manage injuries in snakebite envenomation. Therefore, the aim of this study was to address this gap by characterizing the hemotoxic, myotoxic, and inflammatory profiles of *C. rhodostoma* and *T. insularis* venoms in mice model. By evaluating the impact of varying venom concentrations on hematological parameters, insulin-like growth factor 1 (IGF-1) levels, and histopathological alterations, this study sought to enhance our understanding of the toxicological profiles of these venoms, which could inform the development of more targeted antivenom therapies and improve clinical management of snakebite victims in Indonesia.

Methods

Study design and setting

This study employed an experimental design to evaluate the hemotoxic, myotoxic, and inflammatory effects of *C. rhodostoma* and *T. insularis* venoms in a murine model. The research was carried out over six months at the Laboratory of Animal Physiology, Faculty of Biology, Universitas Gadjah Mada, Yogyakarta, Indonesia. A post-test-only design was implemented to evaluate both systemic and localized effects of the venoms on hematological parameters, plasma IGF-1 levels, and histopathological alterations. All experimental procedures were conducted following standard laboratory protocols and guidelines to ensure the reliability and reproducibility of the results.

Experimental animals

The study utilized 50 male BALB/c mice, aged 7–8 months, with an average weight of 32.7±2.1 g. The animals were procured from Universitas Gadjah Mada, Yogyakarta, Indonesia, and housed under standard laboratory conditions, including a temperature-controlled environment (22–24°C) with a 12-hour light-dark cycle and *ad libitum* access to a standard diet and bi-distilled water. Animals were acclimated to these conditions for seven days prior to the experiment to minimize stress and ensure consistent baseline physiological parameters. Exclusion criteria were implemented to ensure the reliability of the results: mice exhibiting signs of illness, abnormal behavior, or significant deviations in body weight (>10% above or below the average weight range) during the acclimation period were excluded from the study.

Snake venoms

Venom samples were obtained from adult *C. rhodostoma* and *T. insularis*. The snakes were captured in Yogyakarta, Indonesia, and maintained at the Laboratory of Animal Systematics, Faculty of Biology, Universitas Gadjah Mada, Indonesia. Venom extraction was conducted

manually by inducing the snakes to bite into a sterilized collection apparatus equipped with a parafilm-sealed container to collect the venom. The collected venoms were immediately transferred to sterile tubes, frozen at -80°C to preserve bioactivity, and subsequently lyophilized to remove water content. The lyophilized venom was then stored at -20°C in airtight containers to ensure long-term stability and prevent degradation until further use in the study.

In vivo study

Following the acclimation period, the animals were divided into two sets of five treatment groups, one set for each venom (*C. rhodostoma* and *T. insularis*). Each venom was tested independently, with the treatment groups for each venom as follows: saline (negative control), 20 µg, 40 µg, 80 µg, and 100 µg of venom. Each group consisted of five animals, making a total of 25 animals per venom. Ketamine and xylazine were administered at a dose ratio of 10:1 (0.1 mL/100 g body weight) via intramuscular injection to induce anesthesia. Once anesthetized, the mice received an intramuscular injection (100 µL) of the specified venom concentration or saline into the right quadriceps muscle. After six hours, euthanization was performed using an overdose of ketamine and xylazine (200 mg/kg and 20 mg/kg, respectively), administered intramuscularly ensuring humane euthanasia. Following euthanasia, blood samples were collected via exsanguination from the inferior vena cava using a 1 mL syringe and immediately transferred to 3 mL microtubes containing EDTA to prevent coagulation. After blood collection, the right quadriceps muscle was excised and preserved in 10% neutral buffered formalin (NBF) for further histological examination.

Hematological profile analysis

The hematological parameters, including platelets, mean corpuscular volume (MCV), leukocytes, lymphocytes, platelet distribution width (PDW), and plateletcrit were analyzed using a hematology analyzer (Sysmex XP-100, Sysmex Corporation, Kobe, Japan).

IGF-1 plasma quantification

Blood plasma was separated by centrifugation (2500 rpm; 20 minutes; 4°C) and stored at -20°C for subsequent IGF-1 quantification. IGF-1 levels were measured using the ELISA method with a commercial mouse IGF-1 ELISA Kit (E0037Mo, Bioassay Technology Laboratory, Shanghai, China). The assay was conducted according to the manufacturer's instructions.

Histological analysis

Histological examination was performed on the right quadriceps muscle tissues obtained from three animals randomly selected from each group. The analysis focused on the injection site to accurately assess the localized effects of the venom on muscle tissue structure and inflammatory responses. Muscle tissue was processed using the paraffin wax embedding method and stained with hematoxylin and eosin. The extent of edema and inflammatory infiltrate induced by the venom was assessed quantitatively, while muscle degeneration (myonecrosis) was evaluated both quantitatively and semi-qualitatively. For the semi-qualitative analysis of muscle degeneration, an arbitrary scale was employed: 1 (mild) = 0–25% damage; 2 (moderate) = 26–50% damage; 3 (intense) = 51–75% damage; 4 (severe) = 76–100% damage. Muscle histology samples were examined using an Olympus CX33 optical microscope (Olympus Corporation, Tokyo, Japan) with magnifications of 10× (for edema and muscle degeneration) and 40× (for inflammatory infiltrates), coupled with an OptiLab camera (Miconos, Yogyakarta, Indonesia). Image analysis was conducted using OptiLab Viewer version 4.0 (Miconos, Yogyakarta, Indonesia) and ImageJ version 1.54k (National Institutes of Health, Bethesda, USA). The degree of muscle degeneration was averaged from three microscopic fields per preparation, with each group's mean value representing the overall damage score [50,51].

Statistical analyses

Quantitative data were presented as mean ± standard deviation (SD) for hematological profiles, edema, inflammatory infiltration, and plasma IGF-1 levels. Semi-qualitative data analysis for muscle degeneration was scored using a modified arbitrary scale [50]. The normality of the data, including hematological parameters, IGF-1 levels, edema, inflammatory infiltration, and muscle

degeneration, was assessed using the Shapiro-Wilk test. For normally distributed data, one-way ANOVA was used to compare means between groups, followed by Duncan's post-hoc test for multiple comparisons to identify specific pairwise differences. For non-normally distributed data, Kruskal-Wallis's test was employed to assess differences between groups, followed by Dunn's post-hoc test to pinpoint significant pairwise differences [51]. Statistical significance was set at $p<0.05$. Data analysis was performed using SPSS software version 25.0 (IBM, New York, USA).

Results

Hemotoxic effects of *C. rhodostoma* venoms

The hematological profiles of mice exposed to different doses of *C. rhodostoma* venom (20–100 µg) compared to the control group (saline, 0 µg) are presented in **Figure 1**. The results indicated a dose-dependent increase in leukocyte counts (**Figure 1A**), with the highest dose of venom (100 µg) significantly elevating leukocyte levels compared to the control group, suggesting an inflammatory response. Although lymphocyte counts showed a non-significant increasing trend with higher venom doses, the highest values were observed at 100 µg (**Figure 1B**), indicating potential lymphocyte activation or redistribution. MCV remained relatively stable across all venom doses (**Figure 1C**), showing no significant differences from the control, suggesting that red blood cell size was not markedly affected by venom exposure. Platelet counts were significantly reduced in the 20 µg venom group compared to the control (**Figure 1D**), with less pronounced reductions at higher venom doses (40–100 µg), indicating a potential dose-dependent pattern in platelet consumption or sequestration. PDW was significantly increased in groups treated with 40 µg of venom and above (**Figure 1E**), reflecting increased variability in platelet size, which may be associated with ongoing platelet activation or heterogeneity under venom-induced stress. Plateletcrit was significantly reduced at all venom doses compared to the control (**Figure 1F**), with the most considerable decrease observed at 20 µg and slightly higher values at 40–100 µg, indicating a consistent reduction in overall platelet mass.

Hemotoxic effects of *T. insularis* venoms

The hematological profiles of mice treated with varying doses of *T. insularis* venom (20–100 µg) compared to the control group (saline, 0 µg) are presented in **Figure 2**. The leukocyte count exhibited a non-significant increase across all venom doses, with the highest count observed at 100 µg, suggesting a mild inflammatory response without statistical significance (**Figure 2A**). Lymphocyte counts remained relatively unchanged across the venom-treated groups compared to the control, indicating that *T. insularis* venom did not significantly alter lymphocyte levels within the studied dose range (**Figure 2B**). MCV also showed no significant variation among the groups, suggesting that red blood cell size was unaffected by the venom exposure (**Figure 2C**). Platelet counts were generally consistent across all treatment groups, showing no significant reduction or increase compared to the control, implying that *T. insularis* venom did not substantially affect platelet numbers (**Figure 2D**). However, PDW was significantly elevated in the 40 µg venom group compared to the control, indicating increased variability in platelet size, potentially due to platelet activation or heterogeneity in response to venom (**Figure 2E**). Plateletcrit showed no significant changes across all venom doses, indicating that the overall platelet mass was maintained despite venom exposure (**Figure 2F**).

Effects of *C. rhodostoma* and *T. insularis* venom exposures on plasma levels of IGF-1

The plasma levels of IGF-1 in mice treated with *C. rhodostoma* venom at doses ranging from 20 to 100 µg compared to the control group (saline, 0 µg) are presented in **Figure 3A**. The results indicated that IGF-1 levels remained relatively stable across all venom-treated groups, with no significant differences observed compared to the control group. The mean IGF-1 concentrations in all treatment groups were comparable, suggesting that *C. rhodostoma* venom, at the doses tested, does not significantly impact circulating IGF-1 levels in mice. The plasma IGF-1 levels in mice exposed to *T. insularis* venom at doses of 20 to 100 µg, compared to the control group (saline, 0 µg) are presented in **Figure 3B**. The results revealed a significant decrease in IGF-1

levels in venom-treated groups compared to the control, with the most notable reductions observed at 80 and 100 µg. IGF-1 levels in the 20 and 40 µg groups were intermediate, showing no significant difference from either the control or higher venom doses, indicating a potential dose-dependent trend in IGF-1 suppression.

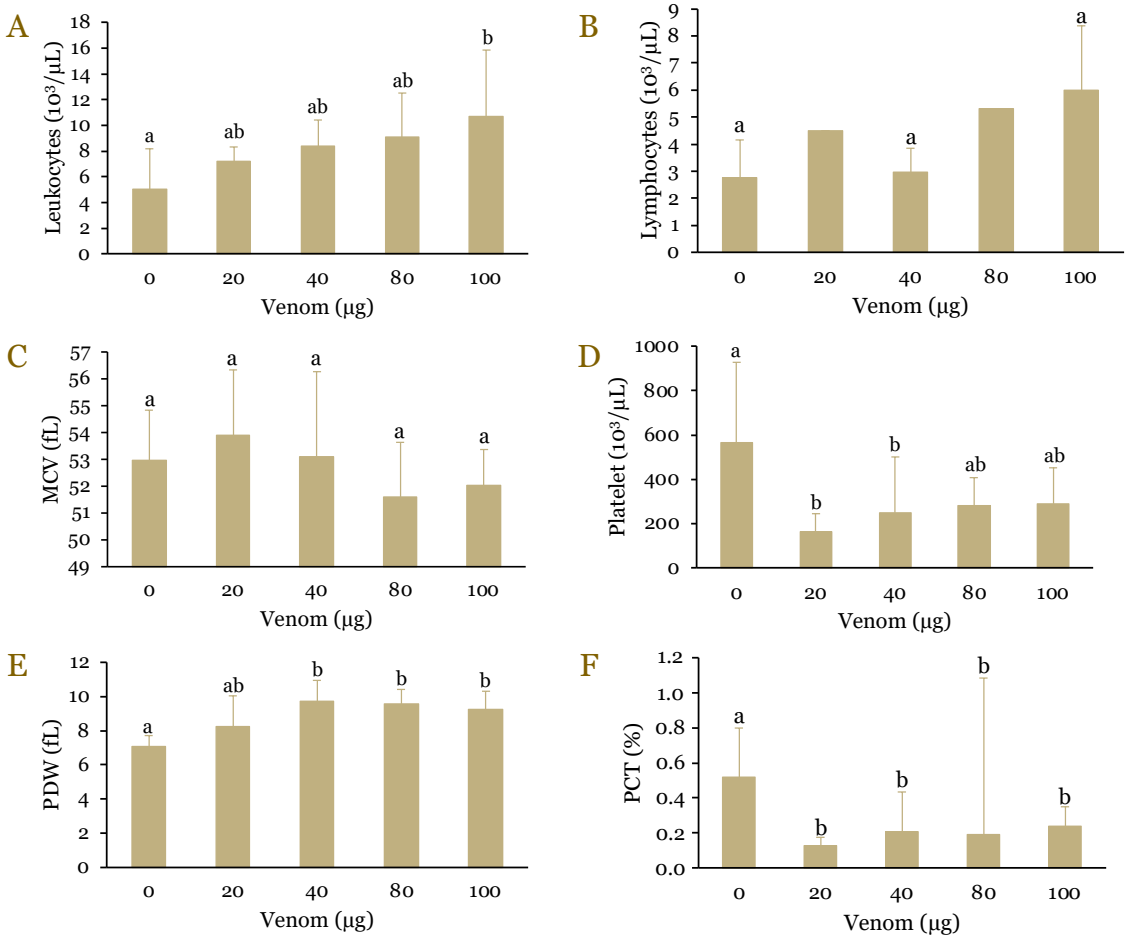

Figure 1. Hematological profiles of mice exposed to *Calloselasma rhodostoma* venom. Panels illustrate the effects of varying doses of *C. rhodostoma* venom (20–100 µg) on leukocyte count (A), lymphocyte count (B), mean corpuscular volume (MCV) (C), platelet count (D), platelet distribution width (PDW) (E), and plateletcrit (PCT) (F) compared to the control group (saline, 0 µg). Data are presented as mean ± standard deviation. Different letters above the bars indicate statistically significant differences between groups ($p<0.05$).

Myotoxic effects of *C. rhodostoma* and *T. insularis* venoms

The edema effects of *C. rhodostoma* venom on muscle tissue, as shown by histological images of quadriceps muscle and the quantification of muscle cell bundle areas, are presented in **Figure 4**. Histological analysis revealed that venom-treated groups (20–100 µg) exhibited marked edema, characterized by increased separation between muscle fibers, indicated by arrows, compared to the tightly packed fibers in the control group (0 µg) (**Figure 4A**). This edema is evidenced by enlarged interstitial spaces and disrupted muscle architecture, reflecting the venom's inflammatory impact on muscle tissue. Quantitative measurements of the muscle cell bundle area indicated a significant increase in treated groups, with the highest values observed at 100 µg ($p<0.05$) (**Figure 4B**). Specifically, muscle cell bundle areas increased progressively with higher venom doses, showing significant differences at 20 µg and further enlargement at 40 µg and above, compared to the control (**Figure 4B**).

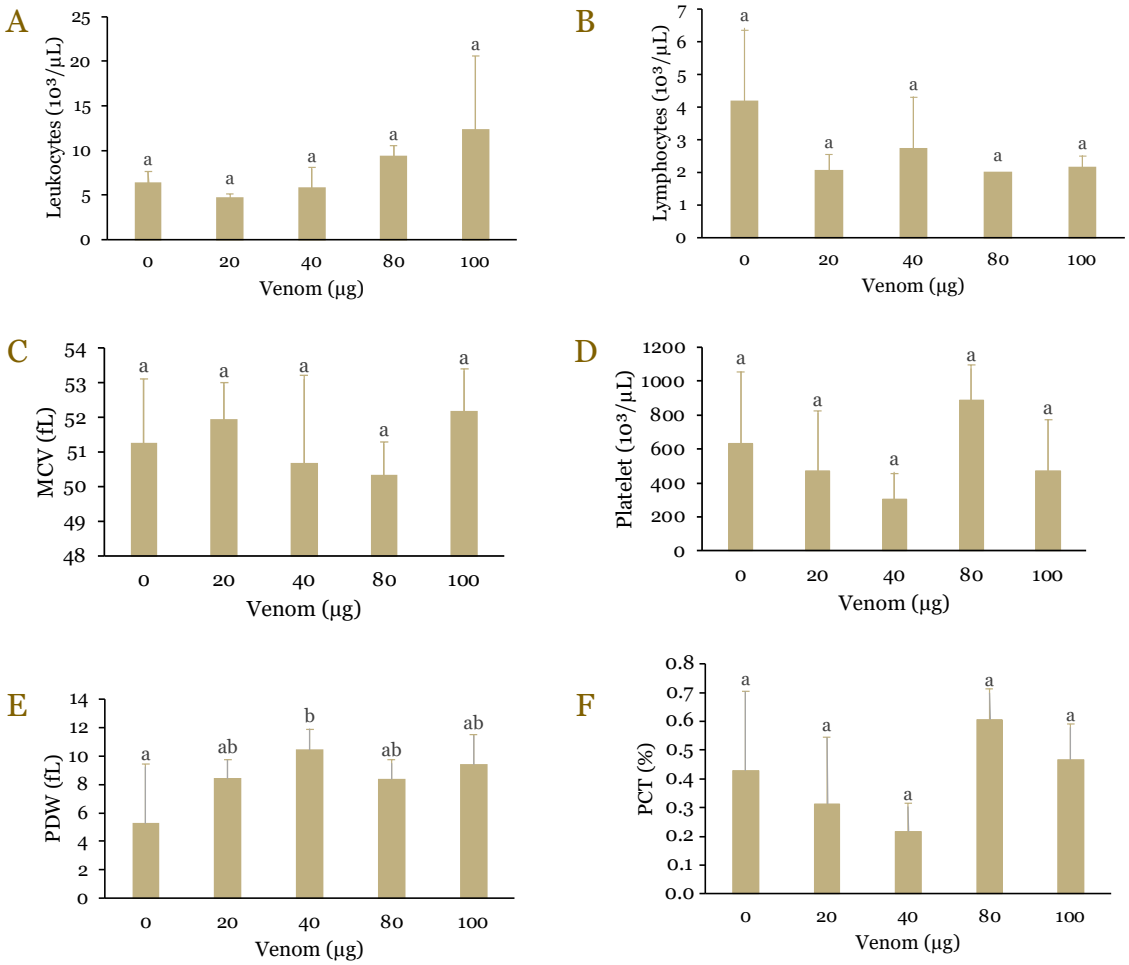

Figure 2. Hematological profiles of mice exposed to *Trimeresurus insularis* venom. Panels illustrate the effects of various doses of *T. insularis* venom (20–100 µg) on leukocyte count (A), lymphocyte count (B), mean corpuscular volume (MCV) (C), platelet count (D), platelet distribution width (PDW) (E), and plateletcrit (PCT) (F) compared to the control group (saline, 0 µg). Data are presented as mean ± standard deviation. Different letters above the bars indicate statistically significant differences between groups (p<0.05).

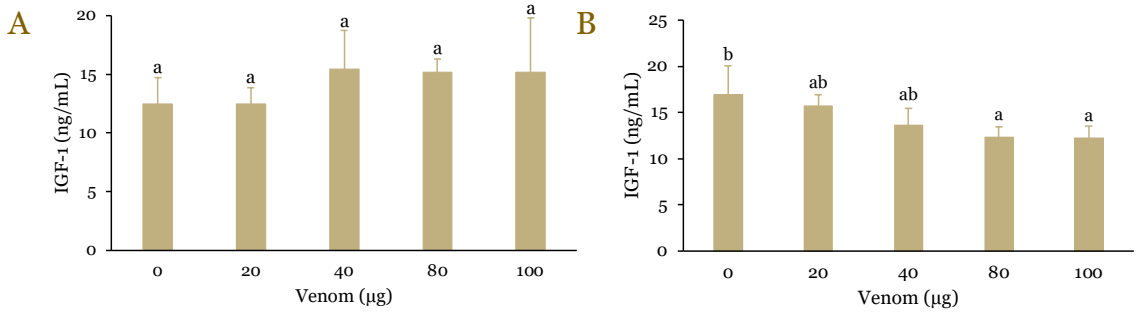

Figure 3. Plasma levels of insulin-like growth factor 1 (IGF-1) in mice exposed to *Calloselasma rhodostoma* (A) and *Trimeresurus insularis* (B) venom. Data are presented as mean ± standard deviation. Different letters above the bars indicate statistically significant differences between groups (p<0.05).

The edema effects of *T. insularis* venom on muscle tissue, as demonstrated by histological preparations and the quantification of muscle cell bundle area in the quadriceps muscle of mice treated with saline (control) and various doses of venom (20–100 µg) are also presented in **Figure 4**. The histological images reveal significant edema in the venom-treated groups, particularly at higher doses, as indicated by the arrows pointing to the increased spaces between muscle fibers (**Figure 4A**). This edema is characterized by the expansion of interstitial spaces and the disruption of normal muscle architecture, which is more pronounced in the 80 and 100

µg venom groups. Quantitative analysis of the muscle cell bundle area supports these observations, showing a dose-dependent increase in bundle size (**Figure 4C**). The 100 µg venom group displayed the largest cell bundle area, significantly greater than the control and lower dose groups. Even at 20 µg, there was a noticeable increase in muscle cell bundle area compared to the control, with further significant increases observed at 40 µg and above.

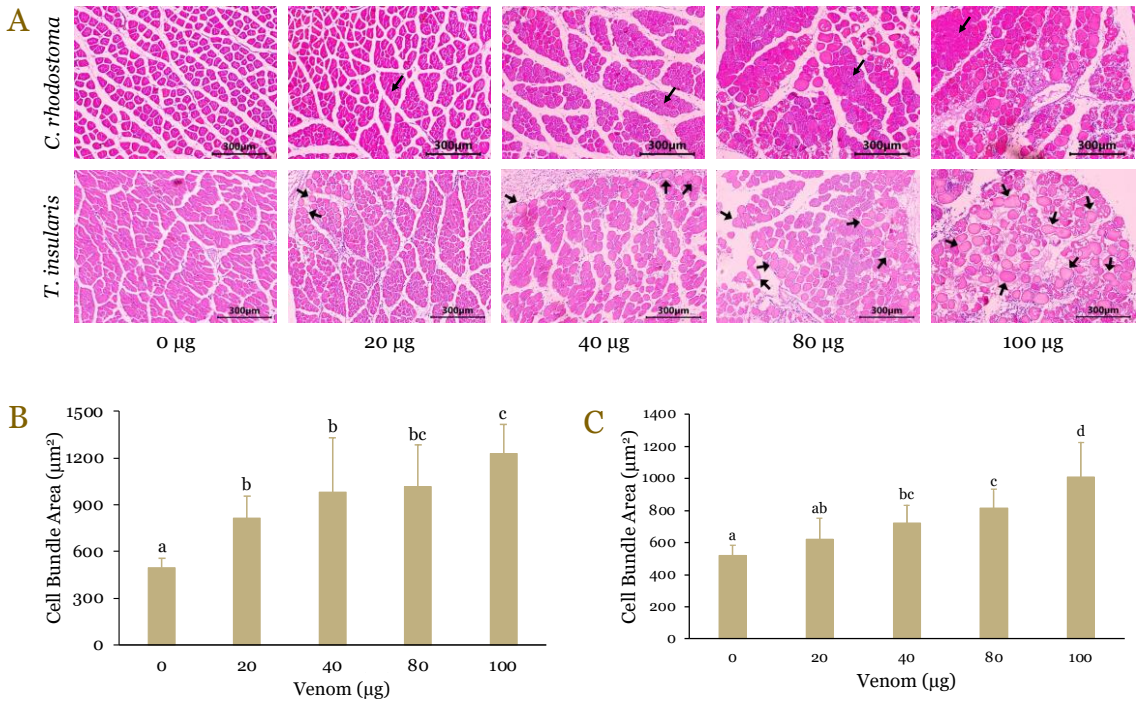

Figure 4. Venom-induced edema in mice treated with *Calloselasma rhodostoma* and *Trimeresurus insularis*. Histological sections of muscle tissue from mice injected with saline (0 µg, control) or escalating doses of venom (20–100 µg) from *C. rhodostoma* (top panel) and *T. insularis* (bottom panel) (A). Black arrows indicate areas of edema. Quantitative analysis of muscle cell bundle area (µm²) corresponding to histopathological findings for *C. rhodostoma* (B). Quantitative analysis of muscle cell bundle area (µm²) corresponding to histopathological findings for *T. insularis* (C). Data are presented as mean ± standard deviation. Different letters above the bars indicate statistically significant differences between groups ($p<0.05$). All histological images were captured at 10× magnification, with a scale bar of 300 µm.

The muscle damage caused by *C. rhodostoma* venom was assessed through histological images (**Figure 5A**) and the quantification of muscle degeneration (**Figure 5B**) in the quadriceps muscle of mice treated with saline (control) and various doses of venom (20–100 µg). Histological analysis revealed progressive muscle degeneration in venom-treated groups, with arrows indicating areas of disrupted and damaged muscle fibers (**Figure 5A**). The control group (0 µg) exhibited intact muscle architecture with minimal signs of damage, whereas venom-treated groups displayed increasing levels of structural disintegration, with the most severe damage observed at 100 µg. Quantitative analysis of muscle degeneration confirms these observations, demonstrating a significant, dose-dependent increase in muscle damage (**Figure 5B**). The percentage of muscle degeneration increased markedly from 20 µg to 100 µg, with the highest degeneration noted in the 100 µg group, which was significantly greater than all other groups. Muscle damage was evident even at the lowest venom dose of 20 µg, and the extent of degeneration continued to escalate with increasing venom concentrations.

The extent of muscle damage induced by *T. insularis* venom and the quantification of muscle degeneration are presented in **Figure 5**. The histological images reveal a progressive increase in muscle degeneration with higher venom doses, as indicated by arrows pointing to areas of disrupted muscle fibers and structural breakdown (**Figure 5A**). The control group (0 µg) displayed well-preserved muscle architecture with minimal damage, while the venom-treated groups showed increasingly severe muscle degeneration, with the most extensive damage

occurring at 80 and 100 µg doses. Quantitative analysis supports these observations, showing a significant, dose-dependent increase in muscle degeneration (**Figure 5C**). The percentage of muscle degeneration rose substantially from the 20 µg dose onwards, with the highest levels observed in the 80 and 100 µg groups, which were significantly greater than the control and lower dose groups. The damage was evident even at the 20 µg dose, indicating the potent myotoxic effect of *T. insularis* venom, which became more pronounced with increasing doses.

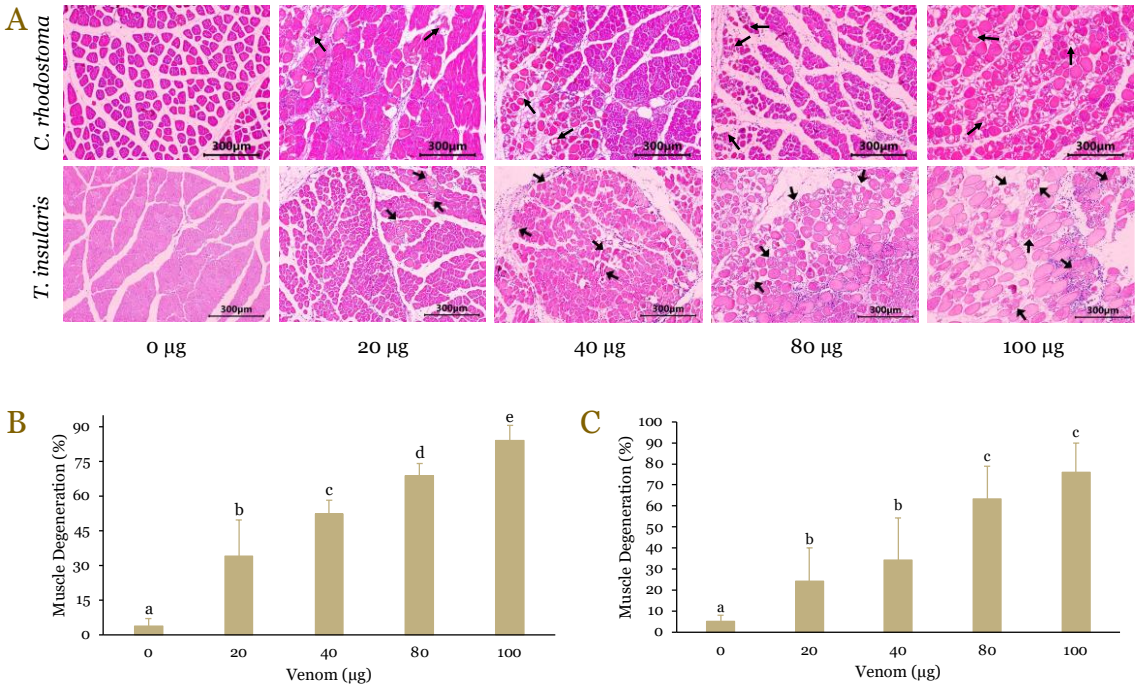

Figure 5. Muscle degeneration in mice induced by *Calloselasma rhodostoma* and *Trimeresurus insularis* venom. Histological images showing muscle tissue from mice treated with saline (0 µg, control) and various doses of venom (20–100 µg) from *C. rhodostoma* (top panel) and *T. insularis* (bottom panel) (A). Black arrows indicate areas of muscle degeneration. Quantification of muscle degeneration percentage corresponding to histopathological findings for *C. rhodostoma* (B). Quantification of muscle degeneration percentage corresponding to histopathological findings for *T. insularis* (C). Data are presented as mean ± standard deviation. Different letters above the bars indicate statistically significant differences between groups ($p<0.05$). All histological images were captured at 10× magnification, with a scale bar of 300 µm.

The inflammatory infiltration and quantification of migrating leukocytes induced by *C. rhodostoma* venom are presented in **Figure 6A** and **6B**. The histological sections reveal increasing infiltration of leukocytes within muscle tissue as venom doses increase, marked by arrows indicating areas of inflammatory cell migration (**Figure 6A**). In the control group (0 µg), leukocyte infiltration was minimal, indicating no significant inflammatory response. In contrast, venom-treated groups showed a dose-dependent rise in the number of leukocyte infiltration, with the most substantial infiltration observed at 100 µg. Quantitative analysis further supports these observations, demonstrating a significant increase in the number of migrating leukocytes as venom doses escalate (**Figure 6B**). The leukocyte count was significantly higher in the 100 µg group compared to all other groups, indicating a robust inflammatory response. Even at the lowest venom dose of 20 µg, there was a noticeable, albeit moderate, increase in leukocyte migration compared to the control. The progressive rise in leukocyte infiltration with higher venom doses reflects the venom's strong pro-inflammatory properties, contributing to localized inflammation and potential muscle tissue damage.

The inflammatory infiltration and the quantification of migrating leukocytes caused by *T. insularis* venom in quadriceps muscle tissue are presented in **Figure 6A** and **6C**. The histological images reveal a gradual increase in leukocyte infiltration with higher venom doses, indicated by arrows marking the presence of migrating inflammatory cells within the muscle tissue (**Figure 6A**). The control group (0 µg) exhibited minimal leukocyte presence, reflecting a

lack of significant inflammatory response. In contrast, venom-treated groups showed increased leukocyte infiltration, with the highest infiltration observed at the 100 µg dose, indicating a pronounced inflammatory reaction. Quantitative analysis of the leukocyte count confirms this trend, showing a significant increase in leukocyte migration in the 100 µg venom group compared to all other groups (**Figure 6C**). The leukocyte counts in the lower dose groups (20–80 µg) remained relatively low and did not differ significantly from the control, suggesting a less intense inflammatory response at these doses. However, the marked rise in leukocyte infiltration at 100 µg highlights the strong pro-inflammatory effect of *T. insularis* venom at higher concentrations.

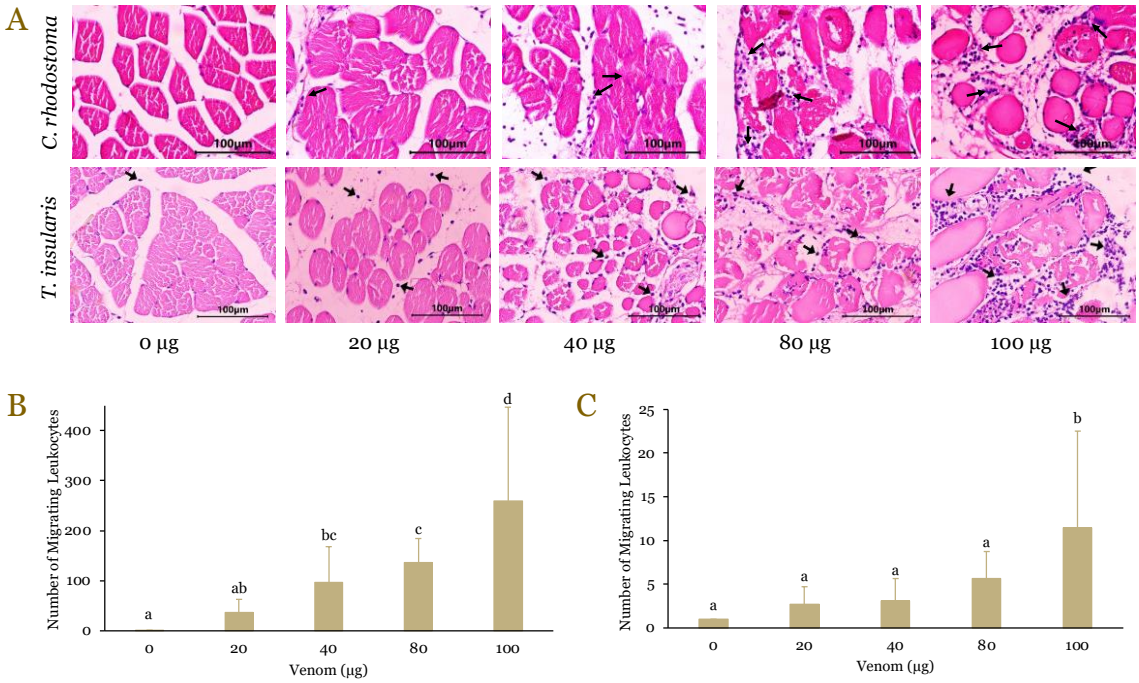

Figure 6. Inflammatory infiltration induced by *Calloselasma rhodostoma* and *Trimeresurus insularis* venom in mice. Histological images of quadriceps muscle from mice treated with saline (0 µg, control) and various doses of venom (20–100 µg) from *C. rhodostoma* (top panel) and *T. insularis* (bottom panel) (A). Black arrows indicate areas of inflammatory infiltration. Quantification of leukocyte counts corresponding to histopathological findings for *C. rhodostoma* (B). Quantification of leukocyte counts corresponding to histopathological findings for *T. insularis* (C). Data are presented as mean ± standard deviation. Different letters above the bars indicate statistically significant differences between groups ($p<0.05$). All histological images were captured at 40× magnification, with a scale bar of 100 µm.

Discussion

The hemotoxic effects of *C. rhodostoma* and *T. insularis* venoms highlighted distinct hematological profiles, suggesting different mechanisms of venom action. *C. rhodostoma* venom induced significant hematological alterations, characterized by a dose-dependent increase in leukocyte counts, indicating a strong inflammatory response, particularly at the highest dose of 100 µg. This leukocytosis, along with the observed increase in PDW and a significant reduction in platelet counts, points towards an inflammatory and hemostatic disturbance likely driven by venom components such as metalloproteinases and phospholipases, which are known to disrupt vascular integrity and activate immune cells. The reduction in plateletcrit and increase in PDW further suggest prominent effects of platelet activation and consumption caused by *C. rhodostoma* venom, leading to potential coagulopathy, a common complication in snakebite envenomation. These findings underscore the potent pro-inflammatory and hemostatic disruptive properties of *C. rhodostoma* venom, which can significantly impact clinical outcomes and complicate treatment, particularly in cases where antivenom availability and administration timing are critical.

In contrast, *T. insularis* venom exhibited a milder hemotoxic profile with only minimal changes in leukocyte counts, suggesting a less pronounced inflammatory response compared to

C. rhodostoma. The lack of significant alterations in lymphocyte counts, MCV, platelet counts, and plateletcrit suggests that *T. insularis* venom does not substantially affect red blood cell or platelet homeostasis within the tested dose range. However, the significant increase in PDW at 40 µg indicates some level of platelet activation or variability, potentially reflecting subtle venom-induced stress on platelet function. The relatively stable hematological parameters suggest that the hemotoxic effects of *T. insularis* venom may be less severe, possibly attributed to differences in venom composition, such as a lower abundance of proteolytic enzymes that directly target blood components. This distinct profile may result in a different clinical presentation in envenomation cases, with potentially less severe bleeding complications compared to *C. rhodostoma*.

Our results provide insights into the differential impact of *C. rhodostoma* and *T. insularis* venoms on circulating IGF-1 levels in mice (**Figure 3**). The IGF-1 levels remained stable across all doses of *C. rhodostoma* venom, indicating that this venom does not significantly alter IGF-1 concentrations in plasma (**Figure 3A**). This suggests that *C. rhodostoma* venom, despite its potent hemotoxic and myotoxic effects, does not directly interfere with systemic factors involved in muscle repair and inflammation, as IGF-1 is a crucial mediator of these processes. The stability in IGF-1 levels might reflect a lack of venom interaction with pathways that regulate IGF-1 production or a compensatory response that maintains homeostasis despite venom exposure. Conversely, *T. insularis* venom exhibited a dose-dependent suppression of IGF-1 levels, with significant reductions observed at the 80 and 100 µg doses (**Figure 3B**). The observed decline in IGF-1 suggests that *T. insularis* venom may negatively influence systemic anabolic and anti-inflammatory pathways, possibly contributing to the muscle damage and impaired healing observed in venom-induced pathology. The decrease in IGF-1 could result from venom-induced systemic inflammation, direct venom action on tissues that regulated IGF-1 or increased catabolic activity overwhelming the anabolic signals mediated by IGF-1. This finding highlights the unique systemic impact of *T. insularis* venom compared to *C. rhodostoma*, indicating that venoms can have distinct physiological effects beyond localized tissue damage. Based on these results, it is recommended to further investigate the specific mechanisms by which *T. insularis* venom reduces IGF-1 levels and to explore whether interventions that stabilize IGF-1 could mitigate venom-induced muscle damage. Additionally, examining other systemic biomarkers related to inflammation and muscle repair could provide a broader understanding of how these venoms affect overall physiological responses.

The present study found significant myotoxic effects of *C. rhodostoma* and *T. insularis* venoms, as evidenced by pronounced edema and structural disruption of muscle tissue in treated groups (**Figure 4**). Both venoms caused marked edema, characterized by increased separation of muscle fibers, enlarged interstitial spaces, and disrupted muscle architecture, suggesting a strong inflammatory response and fluid accumulation in the affected tissues. The quantification of muscle cell bundle areas in both figures showed a clear dose-dependent pattern, with progressive enlargement of the muscle bundles corresponding to increasing venom doses. Notably, the most severe edema was observed at the highest venom doses (80 and 100 µg), indicating that both venoms exert substantial myotoxic effects that worsen with dose escalation. Comparatively, while both venoms demonstrated similar trends in edema formation, *C. rhodostoma* venom appeared to induce slightly more pronounced changes in muscle architecture at lower doses.

Our study also found severe myotoxic effects of *C. rhodostoma* and *T. insularis* venoms, demonstrating their ability to induce significant muscle damage in a dose-dependent manner (**Figure 5**). Both venoms caused progressive muscle degeneration, with structural disintegration becoming more evident at higher doses. In *C. rhodostoma*, the highest venom dose (100 µg) resulted in the most pronounced muscle damage, characterized by substantial fiber disruption and degeneration, indicating the venom's potent myotoxic properties. Similarly, *T. insularis* venom also exhibited strong myotoxic effects, with the most severe muscle damage observed at 80 and 100 µg doses. The comparable patterns of muscle degeneration between the two venoms suggest that both species possess venom components capable of disrupting muscle fiber integrity and inducing severe myonecrosis. The distinct histological changes observed, including muscle fiber breakdown and the enlargement of interstitial spaces, indicate that the venoms' enzymatic

activities likely target the muscle's extracellular matrix, leading to structural weakening and degeneration. Notably, the muscle damage was evident even at the lowest tested doses (20 µg), underscoring the high potency of these venoms at inducing myotoxicity, which poses a significant risk of permanent muscle dysfunction and loss of mobility if not managed promptly.

The present study also demonstrated the ability of *C. rhodostoma* and *T. insularis* venoms to induce inflammatory infiltration within muscle tissue (**Figure 6**). In both venom types, there was a clear dose-dependent increase in the number of migrating leukocytes, suggesting that the inflammatory response intensifies with higher venom doses. Specifically, *C. rhodostoma* venom elicited a robust inflammatory response even at lower doses, with significant leukocyte infiltration noted at 20 µg and escalating sharply at 100 µg. This finding suggests that *C. rhodostoma* venom has strong pro-inflammatory properties that could exacerbate local tissue damage and inflammation. Similarly, *T. insularis* venom also induced inflammatory infiltration, although the response was less pronounced at lower doses (20–80 µg) compared to *C. rhodostoma*. The most substantial inflammatory response to *T. insularis* was observed at 100 µg, where leukocyte migration was significantly elevated compared to all other groups, indicating that higher doses are necessary to trigger a marked inflammatory response. These differences in inflammatory profiles between the two venoms highlight their distinct myotoxic properties, with *C. rhodostoma* potentially causing more immediate inflammatory damage, while *T. insularis* requires higher concentrations to achieve similar effects.

Several studies have investigated the venom composition of *C. rhodostoma*, highlighting its complex and diverse toxic effects [29,52,53]. Early proteomic studies identified 96 distinct proteins, with SVMPs being predominant, and described the roles of toxins such as ancrod and rhodocytin in inducing coagulopathy and platelet aggregation [53]. A combined proteomic analysis using shotgun and gel filtration chromatography further identified 114 proteins from 15 toxin families, including phospholipase A2, SVMP, and serine protease, with novel detections of aminopeptidase and glutaminyl-peptide cyclotransferase [52]. Recently, transcriptome analysis of the venom gland revealed 92 non-redundant toxin transcripts from 16 families, with SVMP, phospholipase A2, and C-type lectin as major contributors to the venom's hemorrhagic and coagulopathic properties [29]. These studies provide insight into the complex biochemical composition of *C. rhodostoma* venom, with a high prevalence of enzymes that target the vascular system and blood components, leading to pronounced hemotoxic and inflammatory effects.

Conversely, studies on *T. insularis* venom have revealed significant biochemical diversity and similarities across different geographic regions [27,32]. A comprehensive analysis of *T. insularis* from eight islands in the Lesser Sunda archipelago, Indonesia, showed consistent venom profiles, with key protein bands identified, including phosphodiesterases, l-amino acid oxidases, P-III SVMP, serine proteases, cysteine-rich secretory proteins, phospholipases A2, and C-type lectins [27]. Additionally, research by Anita *et al.*, [32] compared the venom composition of four *Trimeresurus* species from Indonesia. This study identified 48 proteins across 14 families in *T. insularis* venom, including SVMP, C-type lectin, serine protease, and phospholipases A2 [32], which were present in relatively lower concentrations compared to *C. rhodostoma*. These differences in venom composition, with *T. insularis* showing a lower abundance of highly proteolytic enzymes, may explain the milder hemotoxic and inflammatory effects observed in this study. In contrast, *C. rhodostoma* venom, enriched with SVMPs, phospholipases, and other coagulopathic agents, directly disrupts hemostatic processes and induces strong inflammatory responses. While *T. insularis* venom still contains a range of toxic proteins, it appears to have a reduced impact on blood components, possibly due to lower concentrations of SVMPs and other hemorrhagic toxins.

Taken together, these findings suggest that therapeutic approaches for snakebite envenomation should be tailored according to the specific venom profile of the offending species. For *C. rhodostoma* envenomation, treatment strategies should prioritize managing coagulopathy and inflammation, including early administration of effective antivenom to mitigate platelet consumption and vascular damage. In contrast, for *T. insularis* envenomation, monitoring and managing platelet function and variability might be more relevant, although the overall hemotoxic impact appears less critical.

Conclusion

This study highlights the potent hemotoxic, myotoxic, and inflammatory effects of *C. rhodostoma* and *T. insularis* venoms, demonstrating their capacity to induce significant alterations in hematological profiles, muscle degeneration, and inflammatory infiltration in a dose-dependent manner. *C. rhodostoma* venom exhibited a pronounced impact on blood coagulation and induced stronger inflammatory responses even at lower doses compared to *T. insularis*, which required higher concentrations to produce similar effects. The marked suppression of IGF-1 levels by *T. insularis* venom further suggests its potential to disrupt systemic anabolic and anti-inflammatory pathways, contributing to muscle damage and impaired healing. These findings underscore the need for species-specific therapeutic approaches in snakebite management, emphasizing early intervention with targeted antivenom strategies tailored to address the unique toxicological profiles of each venom. Future research should explore the molecular mechanisms underlying these effects, investigate alternative therapeutic interventions that stabilize key systemic factors such as IGF-1, and evaluate other systemic biomarkers to gain a comprehensive understanding of the physiological impact of these venoms. This knowledge is crucial for improving clinical outcomes in snakebite victims and enhancing the effectiveness of antivenom therapies.

Ethics approval

All in vivo experimental protocols were strictly adhered to following the guidelines of the Animal Ethics Committee of the Faculty of Veterinary Medicine at Universitas Gadjah Mada, Indonesia (approval number: 1/EC-FKH/int./2024).

Acknowledgments

None to declare.

Competing interests

The authors declare that they have no financial or non-financial conflicts of interest.

Funding

This work was supported by Universitas Gadjah Mada, Indonesia under the Indonesian Collaborative Research (Riset Kolaborasi Indonesia) 2024 grant number 1870/UN1/DITLIT/DITLIT/PT.01.03/2024.

Underlying data

Derived data supporting the findings of this study are available from the corresponding author on request.

Declaration of artificial intelligence use

We hereby confirm that no artificial intelligence (AI) tools or methodologies were utilized at any stage of this study, including during data collection, analysis, visualization, or manuscript preparation. All work presented in this study was conducted manually by the authors without the assistance of AI-based tools or systems.

How to cite

Aphrodita A, Sentono DN, Yudha DS, *et al*. Comparative analysis of hemotoxic, myotoxic, and inflammatory profiles of *Calloselasma rhodostoma* and *Trimeresurus insularis* venoms in mice. Narra J 2025; 5 (2): e1874 - http://doi.org/10.52225/narra.v5i2.1874.

References

1. Gutiérrez JM, Calvete JJ, Habib AG, *et al.* Snakebite envenoming. Nat Rev Dis Primers 2017;3(1):17063.
2. Sofyantoro F, Yudha DS, Lischer K, *et al.* Bibliometric analysis of literature in snake venom-related research worldwide (1933–2022). Animals 2022;12(16):2058.

3. Alangode A, Rajan K, Nair BG. Snake antivenom: Challenges and alternate approaches. Biochem Pharmacol 2020;181:114135.
4. Cruz LS, Vargas R, Lopes AA. Snakebite envenomation and death in the developing world. Ethn Dis 2009;19 Suppl 1:S1-46.
5. Gutiérrez JM, Warrell DA, Williams DJ, *et al.* The need for full integration of snakebite envenoming within a global strategy to combat the neglected tropical diseases: The way forward. PLoS Negl Trop Dis 2013;7(6):e2162.
6. Kasturiratne A, Pathmeswaran A, Wickremasinghe AR, *et al.* The socio-economic burden of snakebite in Sri Lanka. PLoS Negl Trop Dis 2017;11(7):e0005647.
7. Chippaux JP. Snakebite envenomation turns again into a neglected tropical disease!. J Venom Anim Toxins Incl Trop Dis 2017;23(1):38.
8. Gutiérrez JM, Burnouf T, Harrison RA, *et al.* A multicomponent strategy to improve the availability of antivenom for treating snakebite envenoming. Bull World Health Organ 2014;92(7):526-532.
9. Kasturiratne A, Wickremasinghe AR, de Silva N, *et al.* The global burden of snakebite: A literature analysis and modelling based on regional estimates of envenoming and deaths. PLoS Med 2008;5(11):e218.
10. Bolon I, Martins SB, Finat M, *et al.* Impact of snakebite on livestock and livelihood: A neglected issue?. Int J Infect Dis 2019;79:66.
11. Feitosa ES, Sampaio V, Sachett J, *et al.* Snakebites as a largely neglected problem in the Brazilian Amazon: Highlights of the epidemiological trends in the State of Amazonas. Rev Soc Bras Med Trop 2015;48 Suppl 1:34-41.
12. Guile L, Lee A, Gutiérrez JM. Factors associated with mortality after snakebite envenoming in children: A scoping review. Trans R Soc Trop Med Hyg 2023;117(9):617-627.
13. Liblik K, Byun J, Saldarriaga C, *et al.* Snakebite envenomation and heart: Systematic review. Curr Probl Cardiol 2022;47(9):100861.
14. Silva A, Isbister GK. Current research into snake antivenoms, their mechanisms of action and applications. Biochem Soc Trans 2020;48(2):537-546.
15. Sofyantoro F, Septriani NI, Yudha DS, *et al.* Zebrafish as versatile model for assessing animal venoms and toxins: Current applications and future prospects. Zebrafish 2024;21(3):231-242.
16. Gutiérrez J, Solano G, Pla D, *et al.* Preclinical evaluation of the efficacy of antivenoms for snakebite envenoming: State-of-the-art and challenges ahead. Toxins 2017;9(5):163.
17. Sanhajariya S, Duffull S, Isbister G. Pharmacokinetics of snake venom. Toxins 2018;10(2):73.
18. Calvete JJ, Fasoli E, Sanz L, *et al.* Exploring the venom proteome of the Western diamondback rattlesnake, *Crotalus atrox* , via snake venomics and combinatorial peptide ligand library approaches. J Proteome Res 2009;8(6):3055-3067.
19. Ainsworth S, Slagboom J, Alomran N, *et al.* The paraspecific neutralisation of snake venom induced coagulopathy by antivenoms. Commun Biol 2018;1(1):34.
20. Alomran N, Alsolaiss J, Albulescu LO, *et al.* Pathology-specific experimental antivenoms for haemotoxic snakebite: The impact of immunogen diversity on the in vitro cross-reactivity and in vivo neutralisation of geographically diverse snake venoms. PLoS Negl Trop Dis 2021;15(8):e0009659.
21. Adrião AAX, Dos Santos AO, De Lima EJSP, *et al.* Plant-derived toxin inhibitors as potential candidates to complement antivenom treatment in snakebite envenomations. Front Immunol 2022;13:842576.
22. Gómez-Betancur I, Gogineni V, Salazar-Ospina A, *et al.* Perspective on the therapeutics of anti-snake venom. Molecules 2019;24(18):3276.
23. Bourke LA, Zdenek CN, Neri-Castro E, *et al.* Pan-American lancehead pit-vipers: Coagulotoxic venom effects and antivenom neutralisation of *Bothrops asper* and *B. atrox* geographical variants. Toxins 2021;13(2):78.
24. Casewell NR, Jackson TNW, Laustsen AH, Sunagar K. Causes and consequences of snake venom variation. Trends Pharmacol Sci 2020;41(8):570-581.
25. Silva A, Hodgson W, Isbister G. Antivenom for neuromuscular paralysis resulting from snake envenoming. Toxins 2017;9(4):143.
26. Khimmaktong W, Nuanyaem N, Lorthong N, *et al.* Histopathological changes in the liver, heart and kidneys following Malayan pit viper (*Calloselasma rhodostoma*) envenoming and the neutralising effects of hemato polyvalent snake antivenom. Toxins 2022;14(9):601.
27. Jones BK, Saviola AJ, Reilly SB, *et al.* Venom composition in a phenotypically variable pit viper (*Trimeresurus insularis*) across the Lesser Sunda archipelago. J Proteome Res 2019;18(5):2206-2220.
28. Kusuma WA, Fadli A, Fatriani R, *et al.* Prediction of the interaction between *Calloselasma rhodostoma* venom-derived peptides and cancer-associated hub proteins: A computational study. Heliyon 2023;9(11):e21149.

29. Tan CH, Tan KY, Ng TS, *et al.* De novo venom gland transcriptome assembly and characterization for *Calloselasma rhodostoma* (Kuhl, 1824), the Malayan pit viper from Malaysia: Unravelling toxin gene diversity in a medically important basal crotaline. Toxins 2023;15(5):315.
30. Bruserud Ø. The snake venom rhodocytin from *Calloselasma rhodostoma*— a clinically important toxin and a useful experimental tool for studies of C-type lectin-like receptor 2 (CLEC-2). Toxins 2013;5(4):665-674.
31. Warrell DA, Looareesuwan S, Theakston RDG, *et al.* Randomized comparative trial of three monospecific antivenoms for bites by the Malayan pit viper (*Calloselasma rhodostoma*) in Southern Thailand: Clinical and laboratory correlations. Am J Trop Med Hyg 1986;35(6):1235-1247.
32. Anita S, Sadjuri AR, Rahmah L, *et al.* Venom composition of *Trimeresurus albolabris*, *T. insularis*, *T. puniceus* and *T. purpureomaculatus* from Indonesia. J Venom Anim Toxins Incl Trop Dis 2022;28:e20210103.
33. Tan CH, Liew JL, Tan NH, *et al.* Cross reactivity and lethality neutralization of venoms of Indonesian *Trimeresurus* complex species by Thai green pit viper antivenom. Toxicon 2017;140:32-37.
34. Osipov A, Utkin Y. What are the neurotoxins in hemotoxic snake venoms?. IJMS 2023;24(3):2919.
35. Slagboom J, Kool J, Harrison RA, *et al.* Haemotoxic snake venoms: Their functional activity, impact on snakebite victims and pharmaceutical promise. Br J Haematol 2017;177(6):947-959.
36. Hutton R, Warrel DA. Action of snake venom components on the haemostatic system. Blood Rev 1993;7(3):176-189.
37. Isbister G. Procoagulant snake toxins: Laboratory studies, diagnosis, and understanding snakebite coagulopathy. Semin Thromb Hemost 2009;35(01):93-103.
38. Maduwage K, Isbister GK. Current treatment for venom-induced consumption coagulopathy resulting from snakebite. PLoS Negl Trop Dis 2014;8(10):e3220.
39. Gulati A, Isbister GK, Duffull SB. Effect of Australian elapid venoms on blood coagulation: Australian snakebite project (ASP-17). Toxicon 2013;61:94-104.
40. Baldo C, Jamora C, Yamanouye N, *et al.* Mechanisms of vascular damage by hemorrhagic snake venom metalloproteinases: Tissue distribution and in situ hydrolysis. PLoS Negl Trop Dis 2010;4(6):e727.
41. Bjarnason JB, Fox JW. Hemorrhagic metalloproteinases from snake venoms. Pharmacol Ther 1994;62(3):325-372.
42. Alomran N, Chinnappan R, Alsolaiss J, *et al.* Exploring the utility of ssDNA aptamers directed against snake venom toxins as new therapeutics for snakebite envenoming. Toxins 2022;14(7):469.
43. Gutiérrez J, Lomonte B. Phospholipase A2 myotoxins from *Bothrops* snake venoms. Toxicon 1995;33(11):1405-1424.
44. Mebs D, Ownby CL. Myotoxic components of snake venoms: Their biochemical and biological activities. Pharmacol Ther 1990;48(2):223-236.
45. Cintra-Francischinelli M, Caccin P, Chiavegato A, *et al. Bothrops* snake myotoxins induce a large efflux of ATP and potassium with spreading of cell damage and pain. Proc Natl Acad Sci USA 2010;107(32):14140-14145.
46. Harris JB, Cullen MJ. Muscle necrosis caused by snake venoms and toxins. Electron Microsc Rev 1990;3(2):183-211.
47. Ferraz CR, Arrahman A, Xie C, *et al.* Multifunctional toxins in snake venoms and therapeutic implications: From pain to hemorrhage and necrosis. Front Ecol Evol 2019;7:218.
48. Hernández R, Cabalceta C, Saravia-Otten P, *et al.* Poor regenerative outcome after skeletal muscle necrosis induced by *Bothrops asper* venom: Alterations in microvasculature and nerves. PLoS ONE 2011;6(5):e19834.
49. Gutiérrez JM, Escalante T, Hernández R, *et al.* Why is skeletal muscle regeneration impaired after myonecrosis induced by viperid snake venoms?. Toxins 2018;10(5):182.
50. Oliveira JS, Sant'Anna LB, Oliveira Junior MC, *et al.* Local and hematological alterations induced by *Philodryas olfersii* snake venom in mice. Toxicon 2017;132:9-17.
51. Vieira RP, De Andrade VF, Duarte ACS, *et al.* Aerobic conditioning and allergic pulmonary inflammation in mice. II. Effects on lung vascular and parenchymal inflammation and remodeling. Am J Physiol Lung Cell Mol Physiol 2008;295(4):L670-L679.
52. Kunalan S, Othman I, Syed Hassan S, *et al.* Proteomic characterization of two medically important Malaysian snake venoms, *Calloselasma rhodostoma* (Malayan pit viper) and *Ophiophagus hannah* (king cobra). Toxins 2018;10(11):434.
53. Tang ELH, Tan CH, Fung SY, *et al.* Venomics of *Calloselasma rhodostoma*, the Malayan pit viper: A complex toxin arsenal unraveled. J Proteomics 2016;148:44-56.